



Original scientific paper

Received: April 11, 2023
Reviewed: May 19, 2023
Accepted: June 26, 2023

UDC: 911.375:628.29(65)
<https://doi.org/10.2298/IJGI2302139G>



INUNDATION RISK OF SEWERAGE SYSTEM ACCORDING TO THE CONCEPTS OF HAZARD AND VULNERABILITY—CASE OF ALGIERS CITY

Sana Gaya^{1*}, Marzouk Cherrared¹

¹University of Sciences and Technology Houari Boumediene (USTHB), Faculty of Civil Engineering, Geotechnics and Hydraulics Department, Algiers, Algeria; e-mails: gaya_sana@hotmail.fr; cherraredm@gmail.com

Abstract: Algiers city frequently experiences significant flooding during rainy weather due to the overflow of its storm sewer network (SSN). Through modeling, simulation, and field studies, vulnerable points of the network have been identified. These points are classified based on a combined assessment of hazard and vulnerability. Hazard is estimated using the Analytical Hierarchical Process (AHP) method, which considers the return period, overflowing height, slope, elevation, and waterproofing. On the other hand, vulnerability is determined by population density. Risk is determined by multiplying hazard and vulnerability. Additionally, a classification based on the FMECA method's criticality index has been performed to complement the approach. The concordance between the two methods is evaluated using Lin's concordance correlation coefficient (CCC), showing strong agreement. The sensitivity analysis conducted on the models highlights their reliability and robustness, making the obtained results trustworthy and useful for network managers. This analysis aids in effective flood management by allocating resources and interventions to the most vulnerable areas of Algiers city.

Keywords: AHP; FMECA; hazard; vulnerability; flood risk

1. Introduction

Flooding is a significant challenge urban areas face worldwide, posing risks to infrastructure, public safety, and the overall well-being of communities. Algiers, the capital city of Algeria, is no exception to this problem. During periods of rainfall, the city of Algiers frequently experiences severe flooding caused by the overflow of its storm sewer network (SSN). These overflows can be attributed to several factors, with the primary ones being inadequate capacity in certain sections of the network, unregulated urban development, and the growing trend of waterproofing catchment areas. The SSN of the central part of the city of Algiers has been modeled to study its behavior during rainy weather. Modeling has become a crucial tool for effective flood risk management (Mohammed et al., 2021; Obaid et al., 2014). By analyzing the outcomes of the modeling and investigating past incidents of overflow, it has been possible to identify the key areas that are particularly vulnerable to network overflow.

*Corresponding author, e-mail: gaya_sana@hotmail.fr

The objective of the study is to create a straightforward yet efficient methodology that relies on minimal data in order to help network managers classify sensitive areas. The classification of these sensitive areas constitutes an important element in the flood risk management strategy since it makes it possible to define the intervention priorities in the management of the sanitation network. The main novelty of this study was the simultaneous utilization of multi-criteria decision-making, cartography, and digital simulation techniques. It is important to note that no similar studies had been conducted for Algiers city before. To enhance the credibility of our results, we used two methods, thus ensuring a comprehensive and trustworthy outcome.

The first is based on the concepts of hazard and vulnerability. The hazard is defined by the return periods (model input) and the overflow heights resulting from the simulation results (model output) using the Mike Urban software developed by the Danish Hydraulic Institute (2019). The simulation focuses on two flow processes: hydrological simulation, using single and double linear reservoir models, and hydraulic simulation involving the resolution of Saint Venant equations. Model calibration is conducted based on rainfall-flow measurements obtained during rainy weather conditions. In addition to the two mentioned criteria, we also use slope, elevation, and waterproofing coefficient to quantify the hazard using the Analytical Hierarchy Process (AHP) method. AHP has been widely utilized for evaluating the sustainability of sanitation networks and specifically for assessing flood risks (Benbachir et al., 2022; Benbachir et al., 2020; Fernández & Lutz, 2010; Kazakis et al., 2015), tsunamis (Poursaber & Ariki, 2016), landslides (Ramos et al., 2014), droughts (Ekrami et al., 2016), and seismic risks (Fentahun et al., 2021). Vulnerability is assessed using population density (Cabrera & Lee, 2020).

The second classification approach relies on the utilization of the Failure Mode, Effects and Criticality Analysis (FMECA) method to determine the criticality index. FMECA combines the principles of Failure Mode and Effects Analysis (FMEA) with criticality analysis (CA). Originally developed by NASA and the automotive industry in 1967, FMEA is known for its ease of use and clear interpretability of results. Its effectiveness has been demonstrated across various domains such as nuclear, aerospace, and medical industries (Rassiah et al., 2020; Sharma et al., 2005). In this study, the evaluation of flood risk is represented by a criticality index, which is determined by the integration of three key parameters: hazard, vulnerability, and detectability.

The concordance of the results obtained is checked using Lin's concordance correlation coefficient (CCC), the value of which shows a very good concordance according to Landis and Koch (1977). Both approaches are subjected to a sensitivity analysis to study their stability and robustness.

2. Methodology

2.1. Flood risk assessment

The concept of risk is in itself quite complex, and its definition can vary depending on the field of study (Fischhoff et al., 1984). Risk can be defined as the anticipated losses, encompassing human lives, injuries, property damage, and disruptions to economic activity, resulting from a specific hazard within a defined area and time frame (United Nations Department of Humanitarian Affairs [UNDHA], 1992). Based on mathematical calculations, risk is the product of hazard and vulnerability. The calculation of risk follows Equation 1, as stated in various studies (Kiyong & Jeong-hun, 2019; UNDHA, 1992; Vojtek & Vojteková, 2016).

$$R_i = H_i \cdot V_i \quad (1)$$

Where R_i is Risk at point i , H_i is Hazard at point i , V_i is Vulnerability at point i , $i = 1$ to n , $n =$ number of flood points (FP).

The risk values obtained are converted and transferred on a scale of 10 according to Equation 2 and 3:

$$S_{c_i} = \frac{R_i \cdot 10}{R_{\max}} \quad (2)$$

$$R_{\max} = H_{\max} \cdot V_{\max} \quad (3)$$

where S_{c_i} is Risk score out of 10, R_{\max} is Maximum score of risk, R_i is Risk at point i , H_{\max} is Maximum score of hazard, and V_{\max} is Maximum score of Vulnerability.

2.1.1. Flood hazard assessment

In accordance with previous studies conducted by Leal et al. (2022), Vojtek and Vojteková (2016), Yin et al. (2015), and the United Nations Disaster Relief Coordinator (1991), hazard is defined as the combination of the probability of occurrence (return period) and the magnitude characteristics of a flood, such as overflow height, flow velocity, or discharge duration. Additionally, hazard is influenced by other parameters, including topographic and environmental factors, which affect the extent of the affected area (Wu et al., 2022; Cabrera & Lee, 2020; Nigusse & Adhanom, 2018). This article defines hazard based on the overflow height, return period, slope, elevation, and waterproofing coefficient, using the following Equation (4):

$$H_i = w_i H_{o_i} + w_i T_i + w_i S_i + w_i E_i + w_i C_{w_i} \quad (4)$$

where H_i is hazard at point i , H_{o_i} is overflow height at point i , T_i is return period at point i , S_i is slope at point i , E_i is elevation at point i , C_{w_i} waterproofing coefficient at point i , and w_i are the weight coefficients determined by the AHP method and presented in Table 3.

The overflow height and return period are considered fundamental elements in defining flood hazard, giving them greater significance compared to other parameters. Elevation and slope are two complementary parameters. Indeed, elevation plays a key role in controlling the flow direction (Fernández & Lutz, 2010), while slope influences the speed of runoff water. Nachappa and Meena (2020) and Seejata et al. (2018) estimated that slope is more important than elevation in estimating the flood hazard index and flood risk zone, respectively, while Fernández and Lutz (2010) considered them to have the same degree of importance. Therefore, based on previous research and the localization of flood points, it has been noted that among the 23 flood points with significant overflowing heights (classes 3 and 4), 22 (96%) are located in areas with low slopes. This percentage decreases to 73% for elevation. This leads us to consider that the slope parameter is more important than elevation. Finally, the waterproofing of soils, which has a direct impact on hydrological dynamics, leads to an increase in runoff velocity, resulting in a reduction in the time of concentration and an increase in the flow rate (Nunes & Rosa, 2020).

The behavior of the SSN is simulated using the Mousse algorithm from Mike Urban software. This algorithm allows us to input the return periods and calculate the corresponding overflow heights. Figure 1 illustrates diagram of the SSN simulation. The calibration of the model was done on the basis of rain-flow data carried out for several rain events.

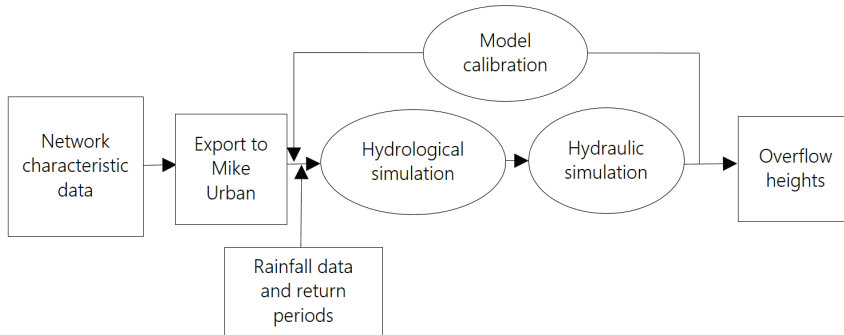


Figure 1. Sewer network simulation diagram.

2.1.2. Vulnerability assessment

There are many definitions of vulnerability, and Nasiri et al. (2016) gave a summarized overview of them. However, it is important to note that we can only meaningfully talk about the vulnerability of a specific system to a specified danger or range of dangers (Brooks, 2003). Vulnerability can be defined as a combination of circumstances resulting from physical, social, and economic factors that increase the community's susceptibility to natural hazards (United Nations International Strategy for Disaster Reduction [UNISDR], 2009).

Furthermore, vulnerability holds utmost importance in the assessment of flood risk, as it determines whether exposure to a hazard poses a significant threat (Nasiri et al., 2016). For example, individuals residing in regions with lower altitudes face greater susceptibility to flood risk compared to those residing in higher elevated areas. The evaluation of flood vulnerability involves assessing the level of susceptibility and exposure of a specific location to flooding events (Danumah et al., 2016). Within the scope of this study, the sole indicator used to assess vulnerability to pluvial flooding is the measure of population density.

2.2. AHP method

The method is based on the comparison of criteria two by two. From the construction of a square matrix (M) of order n , n being the number of criteria (Equation 5), we evaluate the relative importance m_{ij} of a criterion i compared to another j using the judgment scale in Table 1.

$$M = \begin{bmatrix} m_{11} & m_{12} & \dots & m_{1n} \\ m_{21} & m_{22} & \dots & m_{2n} \\ \dots & \dots & \dots & \dots \\ m_{n1} & m_{n2} & \dots & m_{nn} \end{bmatrix}, \quad m_{ii}=1, \quad m_{ji} = \frac{1}{m_{ij}}, \quad m_{ij} \neq 0 \quad (5)$$

Table 1. AHP method judgment scale (Saaty, 1980)

Preference	1	3	5	7	9	2, 4, 6, 8
Defintion	Equally preferred	Lowly preferred	Strongly preferred	Very strongly preferred	Absolutely preferred	Intermediate judgments

The random coherence index (RI) values are calculated based on a sample of 500 randomly generated matrices (Saaty, 1980). For a matrix of order 5, the RI value is determined to be 1.12.

Table 2. Comparison of hazard criteria

Criteria	H_o	E	S	C_w	T
H_o	1	3	2	5	2
E	1/3	1	1/2	2	1/3
S	1/2	2	1	3	1/2
C_w	1/5	1/2	1/3	4	1
T	1/2	3	2	4	1

Table 3. Standardization of hazard criteria

Criteria	H_o	E	S	C_w	T	w
H_o	0.39	0.32	0.34	0.33	0.49	0.38
E	0.13	0.11	0.09	0.13	0.08	0.11
S	0.20	0.21	0.17	0.20	0.12	0.18
C_w	0.08	0.05	0.06	0.07	0.06	0.06
T	0.20	0.32	0.34	0.27	0.27	0.27

With, consistency ratio (CR) = 0.02 < 0.1 and λ_{max} = 5.07; Equation 4 giving hazard therefore becomes Equation 6:

$$H_i = 0.38 H_{o_i} + 0.27 T_i + 0.18 S_i + 0.11 E_i + 0.06 C_{w_i} \quad (6)$$

The procedure for applying the method is illustrated by the flowchart in Figure 2.

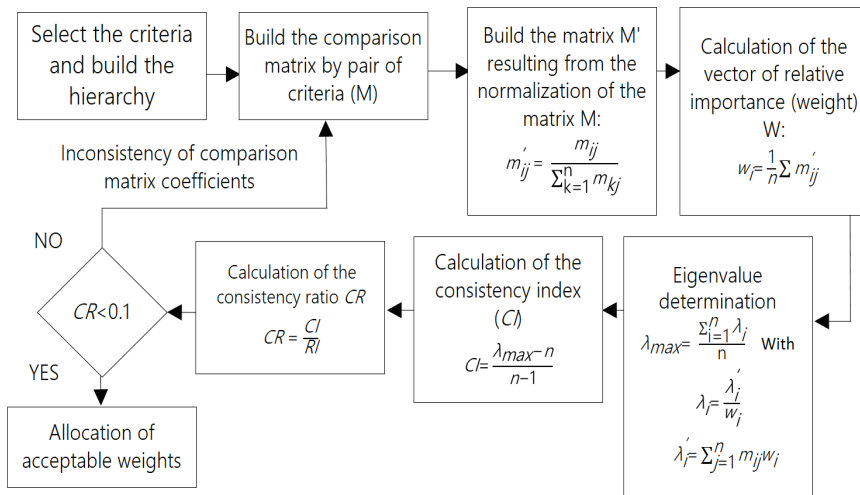


Figure 2. Application step of the AHP method.

2.3. Evaluation of the criticality index (FMECA method)

The FMECA is a method developed to determine potential failure modes in a product or system in order to assess risk before any issues arise (Lipol & Haq, 2011). In this study, the criticality index (IC) is determined based on three parameters: hazard, vulnerability, and detectability. Each parameter is defined by a set of criteria (Figure 3).

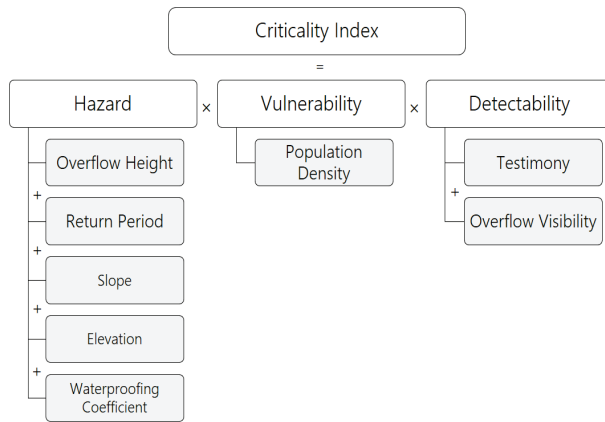


Figure 3. Criticality index calculation flowchart.

For each criterion, specific classes are defined, and scores are assigned accordingly. The scores are assigned in descending order, reflecting the preference for more unfavorable values within each criterion. The overall score for each parameter is calculated using Equation 7:

$$S_c = \sum_{j=1}^n S_{c_j} \quad (7)$$

where, S_{c_j} is the score given to criterion j of the parameter considered, and n is number of criteria.

The product of the three parameters above allows to define a failure criticality index (Equation 8):

$$I_c = S_{c(Hazard)} \cdot S_{c(Vulnerability)} \cdot S_{c(Detectability)} \quad (8)$$

The criticality indices obtained are transformed on a scale of 10, using Equations 9 and 10:

$$S_{c_{I_c}} = \frac{I_c \cdot 10}{I_{c_{max}}} \quad (9)$$

$$I_c = S_{c_{max}(Hazard)} \cdot S_{c_{max}(Vulnerability)} \cdot S_{c_{max}(Detectability)} \quad (10)$$

The criteria for the two parameters, "Hazard" and "Vulnerability", are classified according to Tables 5 and 6, respectively. The classes of the "Detectability" criteria are indicated in Table 4.

Table 4. Criteria and classes of the "Detectability" parameter—Performance scale

Criteria	Classes	Scores
Overflow visibility	Uncrowded area (parking, forest, ravine, etc.)	1
	Fairly frequented area (road, boulevard, etc.)	2
Testimony (residents, etc.)	No	0
	Yes	0.5

3. Results and discussion

3.1. Hazard

The overflow heights from the simulations have been grouped into four classes using the mean and standard deviation method. Each class is assigned a score from 1 to 4 (Table 5). The score increases with higher overflow heights. For each class, a linear equation is calculated based on the class boundaries. This results in four equations, as indicated in Table 5. The purpose of this linear variation is to refine the scores assigned to each class by considering the actual height value obtained at a specific point.

Table 5. Classes of Hazard criteria—Performance scale

Criteria	Weight	Classes	FP Number	Scores	Within-class variation equation
H_o (m)	0.38	0.03–0.13	3	1	$10.22 H_{o_i} + 0.69$
		0.13–0.25	7	2	$7.88 H_{o_i} + 0.99$
		0.25–0.38	13	3	$7.88 H_{o_i} + 0.99$
		0.38–0.51	10	4	$7.79 H_{o_i} + 1.03$
T (years)	0.27	2	15	6	
		5	7	5	
		10	2	4	
		20	2	3	
		50	6	2	
		100	1	1	
S (%)	0.18	0.0028–2.737	16	4	$-0.37 S_i + 4$
		2.737–6.99	13	3	$-0.24 S_i + 3.64$
		6.99–13.82	4	2	$-0.15 S_i + 3.02$
		13.82–38.74	0	1	$-0.04 S_i + 1.55$
E (m)	0.11	0–64	20	4	$-0.0156 E_i + 4$
		64–151	7	3	$-0.01 E_i + 3.74$
		151–231	2	2	$-0.01 E_i + 3.87$
		231–381	4	1	$-0.01 E_i + 2.55$
C_w (%)	0.06	0–24	3	1	$0.04 C_{w_i} + 1$
		24–51	12	2	$0.04 C_{w_i} + 1.11$
		51–75	12	3	$0.04 C_{w_i} + 0.88$
		75–95	6	4	$0.05 C_{w_i} + 0.25$

Note. FP: Flood Points.

Return periods were grouped into six classes (Table 5), with the highest score given to the lowest return period. The score (1 to 6) is higher for shorter return periods. We acknowledge that the range of return periods varies significantly between small values (e.g., two years, five years) and large values (e.g., 50 years, 100 years). However, the impact of overflow is more frequently observed for smaller return periods compared to larger ones. Hence, for simplicity, we have chosen an equal interval rating scale, despite the varying ranges of return periods. The overflow and the return periods of each point, are presented in Figure 4.

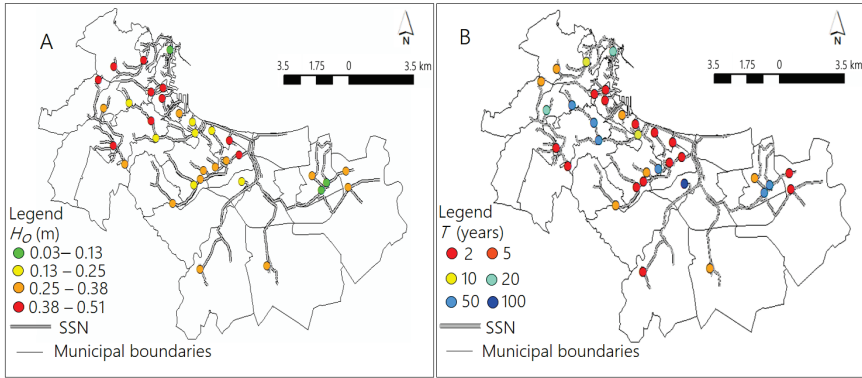


Figure 4. Simulation results: Overflow heights (A) and Return periods (B).

For each point, we retain the height and the return period corresponding to the appearance of the first overflow. Unquestionably the point which overflows for a return period T also overflows for periods greater than T . To estimate and consider the slope, elevation, and waterproofing coefficient parameters, we conducted mapping using ArcMap (Figure 5). The resulting maps were classified using the Jenks (1967) natural breaks method. Each class is assigned a score from 1 to 4 (Table 5).

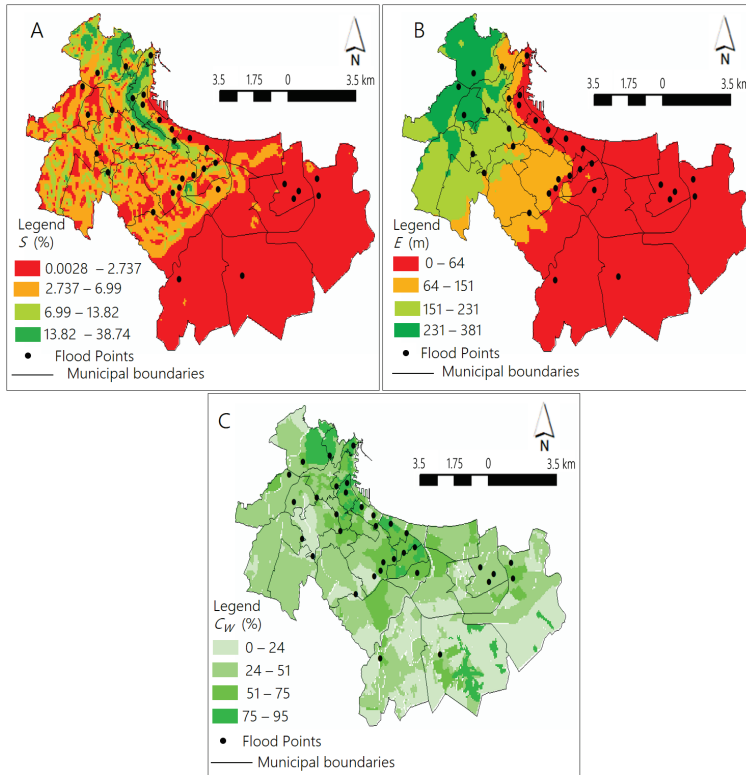


Figure 5. The criteria maps: Slope (A), Elevation (B), and Waterproofing coefficient (C).

The assigned score is higher for areas with lower slope and elevation (indicating higher susceptibility to flooding). Conversely, a higher score was given to areas with higher waterproofing coefficient, indicating a greater potential impact from flooding. Variations within the same class were considered linear. Figure 5 presents maps of slope, elevation, and the waterproofing coefficient, as well as the locations of flood points (black points on the maps).

3.2. Vulnerability

To estimate population density, a map was generated using the ArcMap (Figure 6). The resulting map is divided into four classes using the Jenks (1967) natural breaks method.

Each class is assigned a score ranging from 1 to 4 (Table 6). The areas exhibiting higher population density were assigned the highest scores, signifying a heightened vulnerability to flood-related impacts. On the other hand, areas with low population density were assigned the lowest scores.

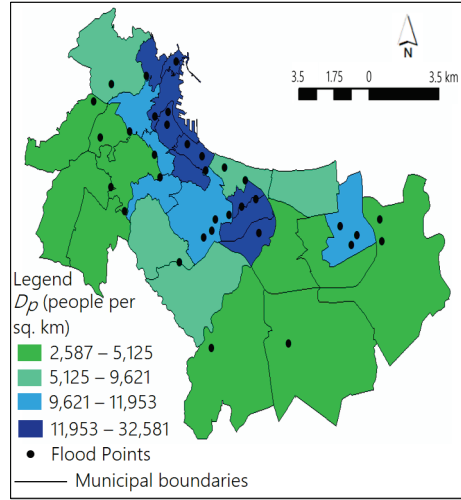


Figure 6. Map of Population density.

Table 6. Classes of vulnerability criteria—Performance scale

Criteria	Classes	FP Number	Scores	Within-class variation equation
D_p (people per sq. km)	2,587–5,125	8	1	$0.00039 D_{p_i} - 0.02$
	5,125–9,621	4	2	$0.00022 D_{p_i} + 0.86$
	9,621–11,953	10	3	$0.00043 D_{p_i} - 1.13$
	11,953–32,581	11	4	$0.00005 D_{p_i} + 3.42$

3.3. Risk and criticality index

The scores obtained for each point, using the two developed methods are summarized in Figure 7. It can be seen that the two graphs have a similar appearance, and in certain areas, they are overlapped. Both methods identify points 4, 10, and 16 as the most critical ones. Point 4 is situated in a densely urbanized area at the city center. The inadequate capacity of the drainage system, combined with a low slope, causes recurring overflows during rainfall events. This significantly disrupts both the daily lives of the population and economic activities, especially given the presence of a bus and train station, as well as a port in the vicinity. Point 10 is located in a low-lying area with a low slope, serving as a crucial route toward the industrial zone in the eastern part of the capital. It experiences frequent flooding events with a 2-year return period. The configuration of the collector at point 16 is unique, as it involves a narrow-sectioned collector installed within the wadi's bed. In various locations, the wadi's bed has been modified to facilitate the passage of specific obstacles, including roads, railways, and urbanized areas which gradually covered the bed of the wadi. Consequently, these areas

experience frequent overflows that are exacerbated by the congestion of the wadi's bed and crossing structures due to the accumulation of substantial amounts of waste.

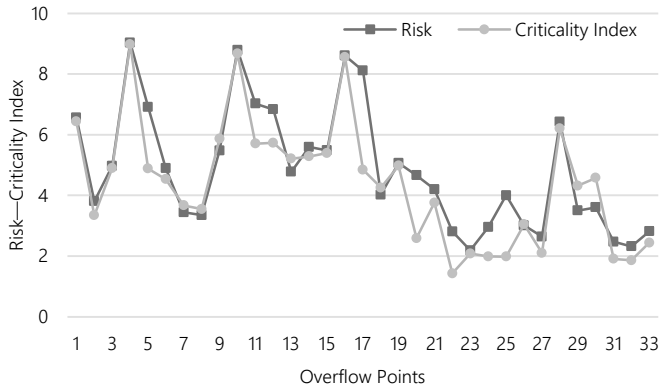


Figure 7. Risk and criticality index results according to overflow points.

To further investigate the agreement between the results obtained from the two methods, the Lin concordance coefficient is calculated. According to Desquilbet (2019), neither the correlation coefficient, nor the leading coefficient of a regression line, or the statistical comparison of the means of the two series may accurately assess the concordance between two sets of measurements. Therefore, one recommended approach is to calculate Lin's CCC introduced by Lin (1989). Lin's CCC is a coefficient ranging from -1 to $+1$, where values closer to $+1$ indicate better concordance, values closer to -1 indicate poorer concordance, and a value of 0 indicates no concordance. The coefficient quantifies the differences between the correlation points of the compared series and the line $Y = X$, which represents perfect concordance (Desquilbet, 2019). Lin's CCC is given by Equation 11:

$$C_C = \frac{2r \cdot s_1 \cdot s_2}{(M_1 - M_2)^2 + s_1^2 + s_2^2} \quad (11)$$

where C_C is Lin's concordance coefficient, r is Pearson's correlation coefficient, M_1 and M_2 are averages of risk and criticality index respectively, s_1 and s_2 are standard deviations of risk and criticality index respectively. The Landis and Koch classification (Desquilbet, 2019; Donner & Eliasziw, 1987) is used to interpret the calculated Lin coefficient.

Table 7. Landis and Koch classification

Lin's CCC	< 0	0–0.20	0.21–0.40	0.41–0.60	0.61–0.80	0.81–1.00
Interpretation	Very bad	Bad	Fair	Mean	Good	Very good

The value of the Lin's CCC calculated between the risk results and the criticality index is equal to 0.88 , indicating a very good concordance according to the scale in Table 7. The determination coefficient, on the other hand, is equal to 0.81 (Figure 8).

4. Model validation—Sensitivity analysis

Sensitivity analysis is the study of the impact of the uncertainties of one or more input variables on the uncertainty of the model output (Pichery, 2014). This analysis is useful because it makes it possible to check the reliability of the used model and to add credibility to obtain results.

4.1. Validation of risk's model

The assessment of the first approach's sensitivity relies on the hazard, given that vulnerability is characterized by a single parameter. To accomplish this, we will adjust the values in the comparison matrix (Table 2) by altering the judgment scale (Table 1) used in the AHP method. By doing so, we can investigate the sensitivity of hazard assessment and observe the resulting effects on the risk scores. The updated comparison matrices, denoted as M_1 to M_3 (of order 5), are presented in Table 8.

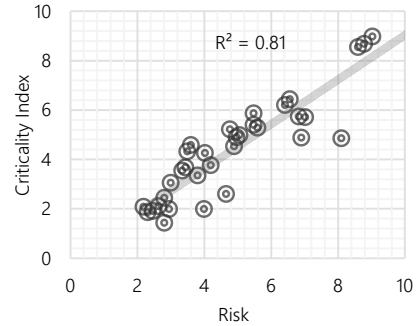


Figure 8. Comparison of R and IC (correlation by the line $Y = X$).

Table 8. M_i comparison matrices of the hazard criteria

Matrix Criteria	M_1					M_2					M_3				
	H_o	E	S	C_w	T	H_o	E	S	C_w	T	H_o	E	S	C_w	T
H_o	1	2	2	5	2	1	3	2	4	2	1	3	2	5	2
E	1/2	1	1	3	1/2	1/3	1	1/2	1	1/2	1/3	1	1/2	2	1/2
S	1/2	1	1	3	1/2	1/2	2	1	2	1/2	1/2	2	1	3	1/2
C_w	1/5	1/3	1/3	1	1/4	1/4	1	1/2	1	1/3	1/5	1/2	1/3	1	1/3
T	1/2	2	2	4	1	1/2	2	2	3	1	1/2	2	2	3	1

The three scenarios that were studied yield hazard (H_s) as expressed by Equations 12 to 14:

$$Hs_{1i} = 0.36 H_{o_i} + 0.26 T_i + 0.16 S_i + 0.16 E_i + 0.06 C_{w_i} \quad (12)$$

$$Hs_{2i} = 0.38 H_{o_i} + 0.25 T_i + 0.17 S_i + 0.11 E_i + 0.09 C_{w_i} \quad (13)$$

$$Hs_{3i} = 0.38 H_{o_i} + 0.24 T_i + 0.19 S_i + 0.12 E_i + 0.07 C_{w_i} \quad (14)$$

where Hs_{1i} , Hs_{2i} , Hs_{3i} , are the hazard resulting from the matrices M_1 , M_2 , M_3 respectively, at point i . The risk Rs , after sensitivity study, is given by Equation 15:

$$Rs_k = Hs_{k_i} \cdot V \quad (15)$$

where $k = 1$ to 3.

The maximum relative difference and the coefficients of determination after sensitivity study depending on hazard are summarized in Table 9.

Table 9. Relative difference and coefficient of determination (influence of hazard)

Series	Maximum relative difference (%)	R^2
R and Rs_1	1.53	
R and Rs_2	1.64	.99
R and Rs_3	1.63	

4.2. Validation of the FMECA model

To study the sensitivity of the second approach based on FMECA, we vary the parameters of slope, elevation, and waterproofing coefficient one by one using the scale in Table 10. The variation results are grouped together in Table 11.

Table 10. Classes and scales of performance for the FMECA model—Sensitivity study

Criteria	Classes	FP Number	Scores	Within-class variation equation
S (%)	0.0028–1.978	10	6	$-0.06 S_i + 2.26$
	1.978–4.864	14	5	$-0.13 S_i + 3.73$
	4.864–8.511	7	4	$-0.19 S_i + 4.65$
	8.511–13.670	1	3	$-0.27 S_i + 5.33$
	13.670–21.578	1	2	$-0.35 S_i + 5.69$
	21.578–38.740	0	1	$-0.51 S_i + 6.01$
E (m)	0–42	17	6	$-0.01 E_i + 3.64$
	42–93	6	5	$-0.02 E_i + 5.41$
	93–152	4	4	$-0.02 E_i + 5.49$
	152–214	2	3	$-0.02 E_i + 5.55$
	214–276	4	2	$-0.02 E_i + 5.82$
	276–381	0	1	$-0.024 E_i + 6$
C _w (%)	0–21	2	1	$0.05 C_{w_i} + 1$
	21–41	7	2	$0.05 C_{w_i} + 0.87$
	41–54	6	3	$0.08 C_{w_i} - 0.24$
	54–65	4	4	$0.09 C_{w_i} - 0.89$
	65–77	9	5	$0.08 C_{w_i} - 0.47$
	77–95	5	6	$0.06 C_{w_i} - 1.69$

Table 11. Relative difference and coefficient of determination (FMECA model)

Criteria	Maximum relative difference %	R ²
S	2.75	.99
E	2.53	
C _w	3.73	

Based on the analysis conducted, it can be concluded that the risk and criticality index values obtained from the two models developed in this study are not significantly influenced by changes in the scores of the criteria. This finding suggests that the models exhibit stability and robustness in their calculations. The fact that the models

are not sensitive to changes in the criteria scores is an important validation step, as it confirms the reliability of the models' outcomes. These findings provide confidence in the models' ability to effectively evaluate and prioritize sensitive areas. Overall, the validation and stability analysis performed on the models demonstrate their reliability and suitability for supporting decision-making processes related to flood risk management.

5. Conclusion

In this study, we used the overflow heights derived from hydrological and hydraulic simulations of Algiers' SSN. Additionally, we incorporated the corresponding return periods for each overflow height, as well as the slope, elevation, and waterproofing coefficients, to assess the level of hazard using the AHP method. This methodology enabled us to

determine the relative importance of each criterion. To evaluate vulnerability, we relied on population density as an indicator, considering the unavailability of other pertinent data.

To ensure the reliability of the risk model employed, we conducted a sensitivity analysis by adjusting the weights assigned to various criteria. We examined the influence of each criterion on the overall risk assessment. The differences in risk scores between the original model and the sensitivity analysis were small, not exceeding 2%. This finding demonstrates the stability and consistency of the risk estimation.

In addition to the risk assessment, we also explored the risk of flooding using the criticality index derived from the FMECA method. This method was chosen due to its recognized reliability and robustness, as evidenced by previous studies referenced in our research. The sensitivity analysis conducted on the criticality index yielded results comparable to the initial risk model, further validating its reliability and effectiveness in assessing flood risk.

The concordance between the flood risks obtained from the two approaches, namely the equation-based risk model and the FMECA model, was evaluated using Lin's CCC, which demonstrated a high level of concordance with a value of 0.88. This indicates a strong agreement between the results obtained from both models, supporting the overall reliability and consistency of our risk assessment framework.

A study has already been conducted on the SSN of Bejaia city by Azoune and Cherrared (2022). They utilized AHP and FMECA methods to classify the overflowing points. The calibration of the results was carried out using an inundation area map established based on past flood events, which is not available for the current case discussed in this paper.

While our study provided valuable insights into flood risk assessment and management, it is important to acknowledge certain limitations. One key limitation is the availability of data. A better understanding of the damaged goods, the condition of buildings, and the precise extent of the affected area enhances the relevance and practical implications of the study. To refine evaluations of flood impact, especially regarding vulnerability, it is essential for future research efforts to prioritize the collection of more comprehensive and detailed data.

This study is part of a global approach which consists of minimizing the failures of the Algiers sewerage network. In particular, managing and reducing flood points (black points). The right intervention strategy would be to start with those that present a greater risk and impact. The solutions should be other than the so-called "conventional" ones. They should be adapted to the specificities of each point by trying to introduce methods which consist in limiting the flow rates of rainwater runoff by alternative techniques (drainage trenches, reuse of roof water, etc.), some of which make it possible to recover rainwater. It would be a welcome resource in an arid country such as ours.

We hope that our study provides a comprehensive framework for flood risk assessment and management in the Algiers sewerage network. The stability, reliability, and concordance of the risk models employed validate their effectiveness in identifying critical zones and guiding intervention strategies.

References

- Azoune, N., & Cherrared, M. (2022). Urban Floods Management Using AHP and FMEA Methods-Case study of Bejaia, Algeria. *Journal of the Geographical Institute "Jovan Cvijic" SASA*, 72(3), 257–271. <https://doi.org/10.2298/IJGI2203257A>

- Benbachir, M., Chenaf, D., & Cherrared, M. (2022). Fuzzy-FMECA Decision-Making Tool for Assessment and Analysis of Performance of Urban Sewerage Networks. *Journal of Pipeline Systems Engineering and Practice*, 13(1), Article 04021078. [https://doi.org/10.1061/\(ASCE\)PS.1949-1204.0000585](https://doi.org/10.1061/(ASCE)PS.1949-1204.0000585)
- Benbachir, M., Cherrared, M., & Chenaf, D. (2020). Managing sewerage networks using both failure modes, effects and criticality analysis (FMECA) and analytic hierarchy process (AHP) methods. *Canadian Journal of Civil Engineering*, 48(12), 1683–1693. <https://doi.org/10.1139/cjce-2020-0287>
- Brooks, N. (2003). *Vulnerability, risk and adaptation: A conceptual framework* (Working Paper No. 38). Tyndall Centre for Climate Change Research.
- Cabrera, J. S., & Lee, H. S. (2020). Flood risk assessment for Davao Oriental in the Philippines using geographic information system-based multi-criteria analysis and the maximum entropy model. *Journal of Flood Risk Management*, 13(2), Article e12607. <https://doi.org/10.1111/jfr3.12607>
- Danish Hydraulic Institute. (2019). *Modelling of storm water drainage networks and sewer collection systems*. <https://manuals.mikepoweredbydhi.help/2019/Cities/CollectionSystem.pdf>
- Danumah, J. H., Odai, S. N., Saley, B. M., Szarzynski, J., Thiel, M., Kwaku, A., Kouame, F. K., & Akpa, L. Y. (2016). Flood risk assessment and mapping in Abidjan district using multi-criteria analysis (AHP) model and geoinformation techniques (cote d'ivoire). *Geoenvironmental Disasters*, 3(12), Article 10. <https://doi.org/10.1186/s40677-016-0044-y>
- Desquilbet, L. (2019). *Guide pratique de validation statistique de méthodes de mesure : répétabilité, reproductibilité, et concordance*. [Practical guide to statistical validation of measurement methods: repeatability, reproducibility, and concordance]. <https://hal.science/hal-02103716v5/document>
- Donner, A., & Eliasziw, M. (1987). Sample size requirements for reliability studies. *Statistics in Medicine*, 6(4), 441–448. <https://doi.org/10.1002/sim.4780060404>
- Ekrami, M., Marj, A. F., Barkhordari, J., & Dashtakian, K. (2016). Drought vulnerability mapping using AHP method in arid and semiarid areas: A case study for Taft Township, Yazd Province, Iran. *Environmental Earth Sciences*, 75, Article 1039. <https://doi.org/10.1007/s12665-016-5822-z>
- Fentahun, T. M., Bagyaraj, M., Melesse, A. M., & Tesfaye, K. (2021). Seismic hazard sensitivity assessment in the Ethiopian Rift, using an integrated approach of AHP and DInSAR methods. *The Egyptian Journal of Remote Sensing and Space Sciences*, 24(3), 735–744. <https://doi.org/10.1016/j.ejrs.2021.05.001>
- Fernández, D. S., & Lutz, M. A. (2010). Urban flood hazard zoning in Tucumán Province, Argentina, using GIS and multicriteria decision analysis. *Engineering Geology*, 111(1–4), 90–98. <https://doi.org/10.1016/j.enggeo.2009.12.006>
- Fischhoff, B., Watson, S. R., & Hope, C. (1984). Defining risk. *Policy Sciences*, 17, 123–139. <https://doi.org/10.1007/BF00146924>
- Kazakis, N., Kougias, I., & Patsialis, T. (2015). Assessment of flood hazard areas at a regional scale using an index-based approach and Analytical Hierarchy Process: Application in Rhodope–Evros region, Greece. *Science of the Total Environment*, 538, 555–563. <https://doi.org/10.1016/j.scitotenv.2015.08.055>
- Kiyong, P., & Jeong-hun, W. (2019). Analysis on distribution characteristics of building use with risk zone classification based on urban flood risk assessment. *International Journal of Disaster Risk Reduction*, 38(3), Article 101192. <https://doi.org/10.1016/j.ijdrr.2019.101192>
- Jenks, G. F. (1967). The Data Model Concept in Statistical Mapping. *International Yearbook of Cartography*, 7, 186–190. <https://www.semanticscholar.org/paper/The-Data-Model-Concept-in-Statistical-Mapping-Jenks/9551c4531a87b4ab01931bf5b68dac945ef3f9ab>
- Landis, J. R. & Koch, G. G. (1977). The Measurement of Observer Agreement for Categorical Data. *Biometrics*, 33(1), 159–174. <https://doi.org/10.2307/2529310>
- Leal, M., Hudson, P., Mobini, S., Sørensen, J., Madeira, P. M., Tesselaar, M., & Zêzere, J. L. (2022). Natural hazard insurance outcomes at national, regional and local scales: A comparison between Sweden and Portugal. *Journal of Environmental Management*, 322, Article 116079. <https://doi.org/10.1016/j.jenvman.2022.116079>
- Lin, I.-K. L. (1989). A Concordance Correlation Coefficient to Evaluate Reproducibility. *Biometrics*, 45(1), 255–268. <https://www.jstor.org/stable/2532051?origin=crossref>

- Lipol, S. L., & Haq, J. (2011). Risk Analysis Method: FMEA/FMECA in the Organizations. *International Journal of Basic & Applied Sciences*, 11(5), 49–57. <https://citeseerx.ist.psu.edu/document?repid=rep1&type=pdf&doi=c933f98700fa61900d6f42a86df98c268740c490>
- Mohammed, M. H., Zwain, H. M., & Hassan, W. H. (2021). Modeling the impacts of climate change and flooding on sanitary sewage system using SWMM simulation: A case study. *Results in Engineering*, 12, Article 100307. <https://doi.org/10.1016/j.rineng.2021.100307>
- Nachappa, T. G., & Meena, S. R. (2020). A novel per pixel and object-based ensemble approach for flood susceptibility mapping. *Geomatics, Natural Hazards and Risk*, 11(1), 2147–2175. <https://doi.org/10.1080/19475705.2020.1833990>
- Nasiri, H., Mohd Yusof, M. J., & Mohammad Ali, T. A. (2016). An overview to flood vulnerability assessment methods. *Sustainable Water Resources Management*, 2, 331–336. <https://doi.org/10.1007/s40899-016-0051-x>
- Nigusse, A. G., & Adhanom, O. G. (2018). Flood Hazard and Flood Risk Vulnerability Mapping Using Geo-Spatial and MCDA around Adigrat, Tigray Region, Northern Ethiopia. *Momona Ethiopian Journal of Science*, 11(1), 90–107. <http://dx.doi.org/10.4314/mejs.v11i1.6>
- Nunes, D. N., & Rosa, L. E. (2020). Compaction and Waterproofing of the Soil In the Urban Fluvial Channels, Mercator. *Mercator*, 19(3), 1–15. <https://doi.org/10.4215/rm2020.e19023>
- Obaid, H. A., Shahid, S., Basim, K. N., & Shreeshivadasan, C. (2014). Modeling sewerage overflow in an urban residential area using storm water management model. *Malaysian Journal of Civil Engineering*, 26(2), 163–171. <https://journals.utm.my/mjce/article/view/15884>
- Pichery, C. (2014). Sensitivity Analysis. In P. Wexler (Ed.), *Encyclopedia of Toxicology* (3rd ed., pp. 236–237). Academic Press. <https://doi.org/10.1016/B978-0-12-386454-3.00431-0>
- Poursaber, M. R., & Arik, Y. (2016). Estimation of Tsunami Hazard Vulnerability Factors by Integrating Remote Sensing, GIS and AHP Based Assessment. *Open Access Library Journal*, 3, Article e2212. <https://doi.org/10.4236/oalib.1102212>
- Ramos, A., Cunha, L., & Cunha, P. P. (2014). Application de la Méthode de l'Analyse Multicritère Hiérarchique à l'étude des glissements de terrain dans la région littorale du centre du Portugal: Figueira da Foz – Nazaré [Analytic Hierarchy Process (AHP) applied to the landslides study in a coastal area of the central Portugal: Figueira da Foz – Nazaré]. *Revue Geo-Eco-Trop*, 38(1), 33–44. http://www.geoecotrop.be/uploads/publications/pub_381_04.pdf
- Rassiah, P., Su, F.-C. F., Huang, Y. J., Spitznagel, D., Sarkar, V., Szegedi, M. W., Zhao, H., Paxton, A. B., Nelson, G., & Salter, B. J. (2020). Using failure mode and effects analysis (FMEA) to generate an initial plan check checklist for improved safety in radiation treatment. *Journal of Applied Clinical Medical Physics*, 21(8), 83–91. <https://doi.org/10.1002/acm2.12918>
- Saaty, T. L. (1980). *The Analytic Hierarchy Process: Planning, Priority Setting, Resource Allocation*. McGraw-Hill.
- Seejata, K., Yodyinga, A., Wongthadam, T., Mahavik, N., & Tantanee, S. (2018). Assessment of flood hazard areas using Analytical Hierarchy Process over the Lower Yom Basin, Sukhothai Province. *Procedia Engineering*, 212, 340–347. <https://doi.org/10.1016/j.proeng.2018.01.044>
- Sharma, R. K., Kumar, D., & Kumar, P. (2005). Systematic failure mode effect analysis (FMEA) using fuzzy linguistic modelling. *International Journal of Quality & Reliability Management*, 22(9), 986–1004. <https://doi.org/10.1108/02656710510625248>
- United Nations Department of Humanitarian Affairs. (1992). *Internationally Agreed Glossary of Basic Terms Related to Disaster Management*. <https://reliefweb.int/report/world/internationally-agreed-glossary-basic-terms-related-disaster-management>
- United Nations Disaster Relief Coordinator. (1991). *Mitigating Natural Disasters: Phenomena, Effects and Options*. Office of the United Nations Disaster Relief Coordinator. <http://cidbimena.desastres.hn/pdf/eng/doc1028/doc1028.htm>
- United Nations International Strategy for Disaster Reduction. (2009). *Terminology on Disaster Risk Reduction*. https://www.preventionweb.net/files/7817_UNISDRTerminologyEnglish.pdf
- Vojtek, M., & Vojteková, J. (2016). Flood hazard and flood risk assessment at the local spatial scale: a case study. *Geomatics, Natural Hazards and Risk*, 7(6), 1973–1992. <https://doi.org/10.1080/19475705.2016.1166874>

- Wu, J., Chen, X., & Lu, J. (2022). Assessment of long and short-term flood risk using the multi-criteria analysis model with the AHP-Entropy method in Poyang Lake basin. *International Journal of Disaster Risk Reduction*, 75, Article 102968. <https://doi.org/10.1016/j.ijdr.2022.102968>
- Yin, J., Ye, M., Yin, Z., & Xu, S. (2015). Review of advances in urban flood risk analysis over China. *Stochastic Environmental Research and Risk Assessment*, 29(3), 1063–1070. <https://doi.org/10.1007/s00477-014-0939-7>